

# Transformative Approaches in Bone Pathology Treatment: The Efficacy of Alendronate-Infused Hydroxyapatite Microspheres

Sarad Pawar Naik Bukke\*, Saswati Mishra, Chandrashekar Thalluri, Cheedipudi Srinivas Reddy, Ananda Kumar Chettupalli, Gali Avinash Kumar

Received: 24 August 2024 / Received in revised form: 14 November 2024, Accepted: 16 November 2024, Published online: 19 December 2024

## Abstract

Alendronate (ALD), when administered orally, has several limitations, including poor bioavailability and gastrointestinal irritation. This study addresses the need for a sustained local delivery system for ALD by fabricating Hydroxyapatite (HA) hollow microspheres using a simple template-directed method with mustard seeds as the template. ALD was adsorbed onto the surface of the HA hollow microspheres at varying concentrations (0.05  $\mu\text{M}$  to 0.2  $\mu\text{M}$ ). The microsphere characteristics properties of the surface and fundamental makeup were examined using a combination of functional group characteristics by Fourier-transform infrared spectroscopy (FTIR), scanning electron microscopy (SEM), and high energetic powder X-ray studies. The cytotoxic effects of the ALD-HA composite were evaluated *In vitro* using the MTT (3-(4,5-dimethylthiazol-2-yl)-2,5-diphenyltetrazolium bromide) assay on fibro sarcoma HTT-1080

cells. Additionally, the drug release capacity of the hollow microspheres was assessed. The findings demonstrate that the hollow ALD-HA microspheres were successfully fabricated and also are a promising desirable action at local sites and designed for bisphosphonates for the management of osteoporosis.

**Keywords:** Alendronate (ALD), Hydroxyapatite, Hollow microsphere, Local drug delivery and Osteoporosis

## Introduction

In the latest developments, the proposal and fabrication of materials exhibiting distinct morphologies have captured significant interest, particularly for their structural and dimensional properties, which contribute to a wide array of exceptional functional characteristics with promising applications (Zhang *et al.*, 2005). Among various hollow structures, those with nanometer and micrometer dimensions have gained substantial popularity. Bio-ceramic hollow microspheres, for example, offer advantageous applications in drug delivery attributed to their encapsulation properties, combining material properties and biological benefits with a large specific surface area (Slowing *et al.*, 2007). Extensive research has been conducted to synthesize inorganic hollow structures, primarily using template-based methods. Hard templates, including microspheres of polystyrene and latex, silica spheres, and nanoparticles of carbon, have been widely employed to prepare hollow microspheres (Daryan *et al.*, 2020). Several studies have also investigated examples of soft templates comprising droplets of emulsion, colloidal micelles, formation of vesicles, and gas-filled bubbles (Umegaki *et al.*, 2020). However, hard-template methods allow for more precise control over the creation of cavities with hollow interiors. The spherical morphology of these microspheres contributes to enhanced bone tissue regeneration, controlled drug release, and reduced inflammatory responses (Thalluri *et al.*, 2023; Sarma *et al.*, 2024; Thalluri, 2024).

An optimal approach for bone regeneration would serve as a localized delivery system, enabling the controlled release of drugs and growth factors while supplying an osteoconductive matrix to facilitate bone formation. Due to their extensive commercial applications—such as encapsulation and drug delivery, catalysis, energy storage, and more—hollow nano-structured microspheres have garnered growing interest from researchers across multiple disciplines (Tamber *et al.*, 2005; Chu *et al.*, 2007; Vasam *et al.*, 2023; Bukke *et al.*, 2024).

### Sarad Pawar Naik Bukke\*

Department of Pharmaceutics and Pharmaceutical Technology, Kampala International University, Western Campus, Ishaka - Bushenyi, Uganda.

### Saswati Mishra

Department of Medical Biotechnology, School of Allied and Healthcare Science, Malla Reddy University, Hyderabad, Telangana, India.

### Chandrashekar Thalluri

Department of Pharmaceutics, Faculty of Pharmaceutical Science, Assam down town University (AdtU), Gandhinagar, Panikhaiti, Guwahati-781026, Assam, India.

### Cheedipudi Srinivas Reddy

Department of Pharmaceutics, School of Pharmacy, Gurunanak Institutions Technical Campus, Ibrahimpatnam, Telangana, India.

### Ananda Kumar Chettupalli

Department of Pharmaceutical Sciences, School of Pharmacy, Galgotias University, Greater Noida, Uttar Pradesh -203201, India.

### Gali Avinash Kumar

Department of Pharmacognosy & Phytochemistry, Sun Institute of Pharmaceutical Education and Research, Kakupalli, SPSR Nellore-524346, Andhra Pradesh, India.

\*E-mail: drsaradpawar@kiu.ac.ug



In particular, the core diameter of these hollow microspheres is crucial, as it dictates the volume of substances that can be encapsulated within the core of the microsphere. Alendronate is an important bisphosphonate used to treat various bone and calcium-related conditions, particularly osteoporosis and Paget's disease. It works by inhibiting the osteoclast-mediated bone resorption process (Sparidans *et al.*, 1998; Orcel & Beaudreuil, 2002; Drake *et al.*, 2008). Compared to other bisphosphonates, alendronate is chemically linked to inorganic pyrophosphate, which serves as a natural regulator of bone turnover (Glorieux, 2007; Cheng *et al.*, 2014). However, pyrophosphates can inhibit the resorption of bone by osteoclasts as well as the mineral incorporation of new bone tissue by osteoblasts (Crotts & Park, 1995). In contrast, alendronate selectively inhibits bone resorption without negatively impacting the mineralization process, making it advantageous over other bisphosphonates.

Hydroxyapatite (HA) has a high structural and compositional similarity to the minerals found in natural bone (Boskey, 2013). This similarity makes HA commonly employed as a biomaterial for bone regeneration as a result of its biocompatibility, bioactivity, osteoconductive attributes, and anti-inflammatory effects. HA-based particles and microspheres have been utilized as carriers for various drugs and proteins (Kuboki *et al.*, 1998; Kumar *et al.*, 2016). Alendronate (ALD) has a strong affinity for  $\text{Ca}^{2+}$  ions in bone tissue, which further establishes HA as an excellent carrier for ALD delivery (Bukke *et al.*, 2024).

This study explores the synergistic combination of Hydroxyapatite (HA) and alendronate (ALD) by hybridizing their properties. We employed a template-assisted synthesis method to fabricate HA hollow microspheres using mustard seeds as a hard template. To enhance the functionality of these microspheres, ALD was adsorbed onto their surface. The cytotoxicity of the resulting microspheres was then assessed in fibro sarcoma HT-1080 cells. ALD is recognized for its effectiveness in treating osteoporosis, but its oral bioavailability remains low. By incorporating ALD on the HA microspheres' surface, a sustained drug delivery approach was achieved, potentially enhancing its therapeutic impact.

## Materials and Methods

Hydroxyapatite (HA) nanoparticles, biocompatible and with a purity greater than 99%, were obtained from Sigma-Aldrich, India. Alendronate Sodium (ALD), a pharmaceutical-grade compound with over 98% purity, was sourced from TCI Chemicals, India. Polyvinyl Alcohol (PVA), an analytical grade substance with 88% hydrolysis and a molecular weight ranging from 30,000 to 70,000 g/mol, was acquired from SRL Chemical Laboratories Private Limited, India. Mustard seeds were purchased from local stores. Ethanol, an ACS reagent grade with 99.5% purity, was collected from Merck, Germany. 7.4 P<sup>H</sup> Phosphate-buffered saline in a sterile form and of molecular biology grade, remained sourced from Thermo Fisher Scientific, USA. Dichloromethane (DCM), with analytical grade and over 99.8% purity, was obtained from Himedia Laboratories, India. Tween 80, also an analytical grade and USP/NF grade for bio-applications, was sourced from Himedia Laboratories, India. Finally, Pluronic F-68 was acquired from Sigma-Aldrich, USA.

## Production of Hollow Microspheres Using a Template Technique

Hollow Hydroxyapatite (HA) microspheres were effectively synthesized using a straightforward, one-step template-directed synthesis method. This approach is recognized as a reliable method to produce hollow structures. The synthesis of these hollow microspheres follows three primary steps: surface modification, precursor attachment, and core removal.

### Step 1. Surface Modification

Initially, mustard seeds (sized 0.3–0.5 mm) were chosen as a hard template due to their suitable size and structure. These seeds underwent surface modification by etching in a sulphuric acid solution for 15 minutes. This treatment enabled better adherence of the HA precursor to the seed surface. After etching, the planted seeds (microspheres) were rinsed thoroughly using fresh water eliminating any residual acid, and allowed to air dry at a specified temperature.

### Step 2. Precursor Attachment

The modified mustard seeds were then dip-coated in a solution containing Hydroxyapatite and a binder mixture (10% gelatin and polyvinyl alcohol, PVA) to ensure a stable and uniform layer. The coated seeds were air-dried at room temperature, and the dip-coating process was repeated twice to achieve a thick, homogeneous HA layer on the surface of each seed.

### Step 3: Core Removal

To create the hollow structure, the coated seeds were subjected to high-temperature sintering. This process involved heating the coated seeds to 1220°C for two hours. During sintering, the mustard seed core was entirely burned away, leaving behind a rigid, hollow HA microsphere. This step not only removed the core but also imparted structural stability to the fabricated microsphere due to the high-temperature treatment (Bukke *et al.*, 2019; Zhou *et al.*, 2021). This simple yet effective method produces robust hollow HA microspheres with potential applications in various fields because of their distinctive structural properties. Finally, the composition of Alendronate-Loaded Hydroxyapatite Hollow microsphere formulations is depicted in **Table 1**.

**Table 1.** Quantification of Alendronate-Loaded Hydroxyapatite Hollow Microspheres formulations F1-F3

Name of the Ingredients/ mg	F1	F2	F3
Hydroxyapatite (HA) (mg)	500	500	500
Alendronate Sodium (ALD) (mg)	0.25	0.5	1.0
Polyvinyl Alcohol (PVA)(mg)	10	10	10
Mustard Seeds (mg)	300	300	300
Ethanol(ml)	50	50	50
Phosphate Buffered Saline (PBS) (ml)	50	50	50
Tween 80 (mg)	5	5	5
Pluronic F-68 (mg)	5	5	5

### Drug Loading on Hollow Microsphere

To evaluate the effectiveness of hollow microspheres as drug carriers, three different concentrations of Alendronate (0.05, 0.1, and 0.2  $\mu\text{M}$ ) were tested. Each concentration was prepared in a separate flask, with 5 mg of hollow microspheres added to each. The flasks were incubated for 12 hours to enable the microspheres to load the drug effectively. After incubation, the Alendronate-loaded microspheres were air-dried overnight and stored in a desiccator for further evaluation. For drug release analysis, the microcapsules were submerged in a phosphate buffer solution set to a pH of 7.4. and incubated. The buffer blend was subsequently the analysis was performed using a UV-visible spectrophotometer at a wavelength of 491 nm. to assess the concentration of free (unbound) Alendronate (Thalluri *et al.*, 2013). The following equation was used for calculation.

$$\begin{aligned} \text{Percentage drug loading (\%)} \\ = (W_a - W_f / W) \times 100 \end{aligned} \quad (1)$$

Where,  $W_a$  - weight of drug-loaded,  $W_f$  - weight of free drug,  $W$  - total weight of drug

### Characterizing the Physicochemical Properties of ALD-HA Composites

#### Particle Size and Shape

The SEM remained employed to examine the hollow microspheres, which were sputter-coated with platinum under vacuum to enhance imaging quality. The surface patterning of the fabricated microspheres was analyzed at the specified amplification at a desired temperature. Additionally, cross-sectioning of the microvesicles enabled the examination of the inner core and measurement of the microsphere wall thickness, providing further structural insights (Thalluri *et al.*, 2014).

#### Elemental Composition Analysis of Alendronate-Loaded Hydroxyapatite (ALD-HA)

To examine the uniform adsorption of Alendronate (ALD) across the entire phase of the CaP microspheres, scanning electron microscopy with field emission technology (FESEM) coupled with spectroscopy for energy dispersive analysis. (EDS), was conducted consuming a Carl Zeiss Supra 55 model equipped with a Gemini column. This analysis confirmed the uniform, even distribution of the calcium (Ca) and phosphorus (P) substratum on the microsphere's external surface, aligning with the stoichiometric ratio characteristic of bone (Yi *et al.*, 2017).

#### Analysis of Alendronate-Loaded Hydroxyapatite (ALD-HA) Composite

The IR overlay spectra of native Alendronate (ALD) and ALD-HA composites at different concentrations (0.05  $\mu\text{M}$ , 0.1  $\mu\text{M}$ , and 0.2  $\mu\text{M}$ ) were analyzed using Fourier Transform Infrared Spectroscopy (FTIR) with a Perkin Elmer instrument. Diffuse reflectance was employed for the analysis, with potassium bromide

(KBr, Merck KGaA) pellets serving as the primary medium. KBr, mixed with the sample, acted as a carrier to facilitate accurate IR spectrum analysis (Srujan *et al.*, 2018).

#### Cytotoxicity of Alendronate-Loaded Hydroxyapatite (ALD-HA) Composite

To assess the cytotoxicity of free Alendronate (ALD) and the ALD + HA composite, cells ( $1 \times 10^6$  cells/mL) were scattered in a 96-well format plate with DMEM and cultured at 5 percentage  $\text{CO}_2$  and  $37^\circ\text{C}$  for 24 hours. Following this initial incubation, the sample cells were subjected to a range of concentrations consisting of free ALD and ALD + HA (0.05  $\mu\text{M}$ –0.2  $\mu\text{M}$ ) and incubated for an additional 24 hours. To evaluate cell viability, each well received the addition of MTT solution containing 0.5  $\mu\text{g/mL}$ , and then the plates were incubated for 2 hours at  $37^\circ\text{C}$  and 5%  $\text{CO}_2$  in darkness. Metabolically active cells reduced MTT to insoluble formazan crystals, producing a dark purple color. The resulting formazan crystals were subsequently liquefied in a dissolving buffer, and absorbance was recorded at 570 nm using an ELISA reader (Lisaquant-TS), and cell viability was determined by comparing the absorbance of the treated samples with that of the untreated control cells (Bukke *et al.*, 2024).

## Results and Discussion

Bioceramic hollow microspheres have shown promising applications as drug carriers due to their unique physicochemical and biological properties. These microspheres offer a high specific surface area, and excellent encapsulation capacity, and are conducive to tissue regeneration. Additionally, they provide controlled and optimized drug release, which helps reduce inflammatory reactions (Zhong *et al.*, 2007; Meldrum & Cölfen, 2008).

Bisphosphonates, such as Alendronate (ALD), represent an important class of drugs associated with calcium and bone-related disorders. These drugs are commonly used in clinical settings for the treatment of bone-related conditions, including osteoporosis—particularly in women—and Paget's disease (Agrawal *et al.*, 2007, 2009). Microsphere-based delivery systems have significantly contributed to the controlled and sustained release of such drugs, enhancing their therapeutic efficacy.

In this present research, hollow microspheres were produced using a template-directed method (Lou *et al.*, 2007; Wu *et al.*, 2008). The microspheres surface morphology and chemical composition were examined using Scanning electron microscopy (SEM) (Yang *et al.*, 2012). SEM images of the surface (**Figures 1a and 1b**) reveal mesoporous, plate-like Hydroxyapatite (HA) particles, with a rough and irregular external surface, which is favourable for cell attachment. Cross-sectional imaging (**Figure 1c**) shows the microsphere wall, consisting of two distinct layers: a highly porous inner layer and a less porous outer layer, with an overall wall thickness of approximately 100  $\mu\text{m}$ .

**Figure 1d** provides a clear view of the internal core of the hollow HA microsphere, showing a smoother internal surface relative to

the outer surface. Following fabrication, the hollow microspheres were dip-coated in various concentrations of ALD solution (0.05%, 0.1%, and 0.2%) for drug loading.

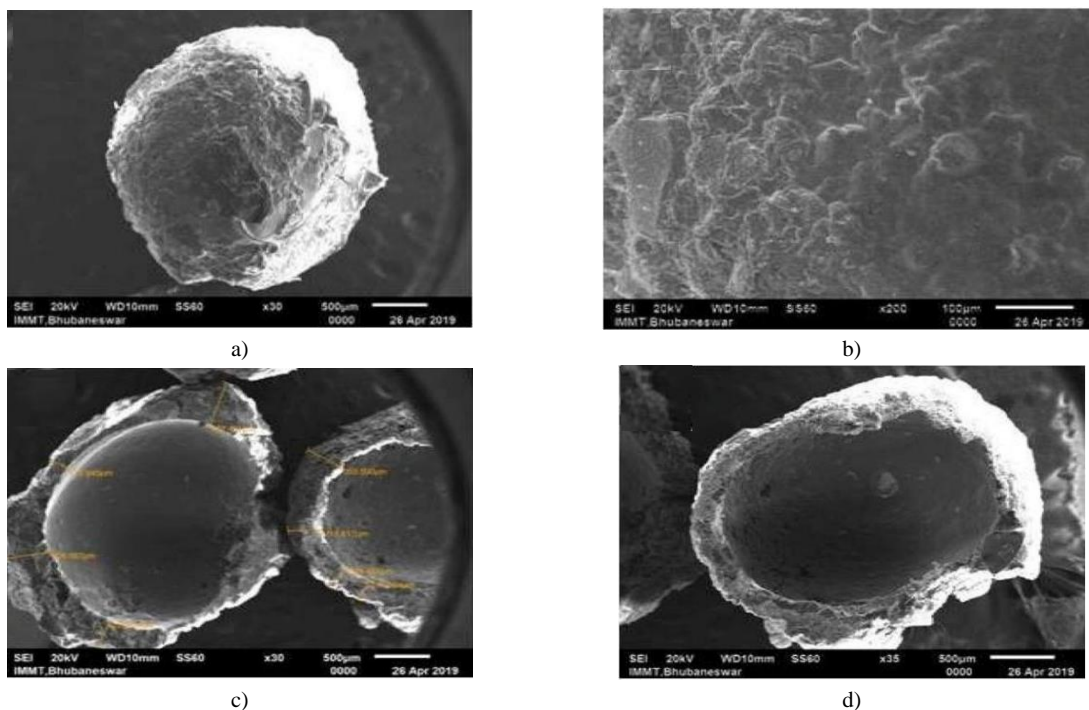


**Figure 1.** SEM images of HA microspheres: a, b) external surface of the hollow HA microsphere; c) cross-section; d) internal view of the core.

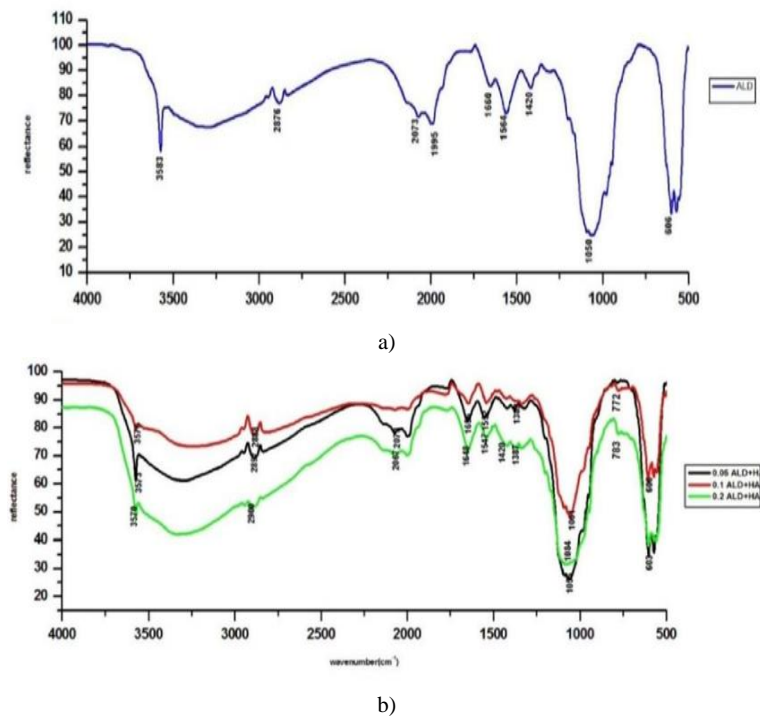


**Figure 2.** A comparative FTIR analysis of ALD and ALD-HA composites of 0.05 μM, 0.1 μM and 0.2 μM

Subsequently, FTIR and energy-dispersive X-ray Spectroscopy analyses were conducted to confirm that the hollow microspheres possessed the composition and structure characteristic of HA-based material loaded with Alendronate (ALD). The FTIR spectra of the prepared ALD-adsorbed microspheres were compared to the control ALD spectrum, as shown in **Figure 2**.

The analysis revealed that a peak corresponding to the wavenumber of  $3570\text{ cm}^{-1}$  was present in all three different concentrations of ALD-loaded HA, with slight deviations:  $3573\text{ cm}^{-1}$  for  $0.1\text{ }\mu\text{M}$  ALD + HA and  $3576\text{ cm}^{-1}$  for  $0.2\text{ }\mu\text{M}$  ALD + HA. These deviations are connected to the vibrations associated with the stretching movements of chemical bonds, specifically the elongation and contraction of the O-H molecules.

Moreover, a wide absorption band observed in the spectrum, typically spanning a range of wavelengths, centered around  $3223\text{ cm}^{-1}$  corresponds to the vibration mode of O-H groups related to hydrogen bonding, which corresponds to incorporated water. The characteristic peak at  $1648\text{ cm}^{-1}$  is observed in all three ALD + HA compositions, indicating the bending vibration of the NH  $\text{cm}^{-1}$  group from the primary amine compound. Another peak at  $783\text{ cm}^{-1}$  is also related to the same primary amine compound. Furthermore, the peak at  $1420\text{ cm}^{-1}$  is allied with carbonate ( $\text{CO}_3^{2-}$ ) ions, while the significant peak at  $1348\text{ cm}^{-1}$  is assigned to the bending of the O-H group. In the ALD-HA composite spectrum, a series of peaks characteristic of the oscillation mode of phosphate ions were also identified.

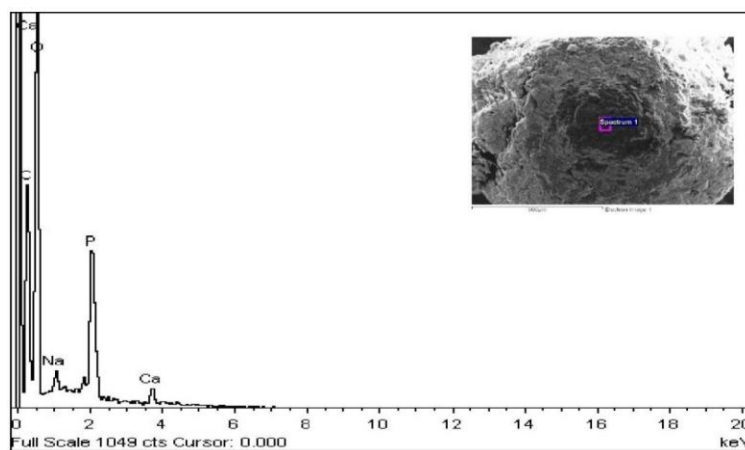


**Figure 3.** Fe-SEM/EDS analysis of the surface of ALD adsorbed hollow HA microsphere

Alendronate (ALD) is recognized for its high binding affinity to calcium phosphate (CaP) phases due to its ionic characteristics. Unlike other bisphosphonates, the anions of ALD are particularly suited for interacting with calcium cations in the CaP phase via bidentate chelation (Josse *et al.*, 2005; Boanini *et al.*, 2007). When ALD adsorbs onto the Hydroxyapatite (HA) microspheres, two potential mechanisms may occur due to Calcium ions interacting with the anionic phosphate groups of ALD as well as with CaP. Precipitates, followed by the incorporation of ALD.

To investigate the uniformity of ALD adsorption throughout the HA microspheres, Field Emission Scanning electron microscopy (FE-SEM) and Energy Dispersive X-ray Spectroscopy (EDX) analyses were conducted, as depicted in **Figure 3** (Wu *et al.*, 2008; Jagyanseni *et al.*, 2023). The EDS analysis indicated the presence of elements including phosphorus (P), calcium (Ca), carbon (C), oxygen (O), and sodium (Na) in the synthesized HA microspheres.

As detailed in **Table 2**, the chemical composition was mapped based on the EDS spectra. Notably, the ratio Ca: Phosphorus of the Hydroxyapatite powder used in the synthesis of the microspheres was calculated to be 1.67, which precisely matches the stoichiometric ratio of pure Hydroxyapatite (Ca/P = 1.67) (Josse *et al.*, 2005).

**Table 2.** Elemental Analysis of the Fabricated Alendronate-Loaded Hydroxyapatite (ALD-HA) Hollow Microspheres

Elements	App Concentrations	Intensity Concentrations	Weight (%)	Weight (%) Sigma	Atomic (%)
<b>C K</b>	2.58	0.8356	35.76	1.21	44.34
<b>O K</b>	4.42	0.9488	54.99	1.20	51.19
<b>Na K</b>	0.11	0.9874	1.27	0.26	0.82
<b>PK</b>	0.72	1.3514	6.25	0.42	3.01
<b>Ca K</b>	0.14	0.9573	1.7	0.22	0.65

This study examined the cytotoxic effects of different concentrations of Alendronate (ALD) and ALD. Combined with Hydroxyapatite (HA) treatment. Previous reports indicated that the HOS cell line, MG-63, exhibits a biphasic response to ALD, with effective stimulation observed at low doses (ranging from  $10\text{ nm}$  to  $10\text{ }\mu\text{M}$ ) and inhibitory effects at higher concentrations (Im *et al.*, 2004; Xiong *et al.*, 2009; Goyal & Kulkarni, 2024). In our findings, we observed that low doses of ALD ( $0.05\text{ }\mu\text{M}$  to  $0.2\text{ }\mu\text{M}$ ) did not

significantly impact cell proliferation in relation to the control as illustrated in **Figure 4**.

After 24 hours of incubation, both free ALD and ALD + HA composites showed no significant cytotoxic effects on HT-1080

cells. These results indicate that low doses of ALD do not adversely affect cell morphology or viability, as demonstrated by the MTT assay.

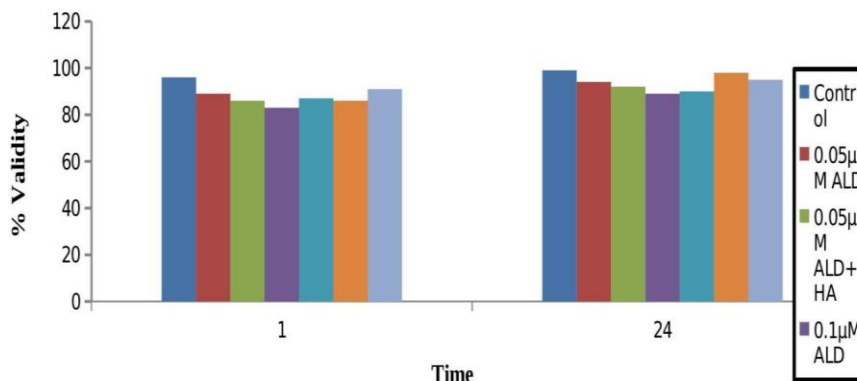


**Figure 4.** Cytotoxicity activity of different concentrations of ALD+HA on HT-1080 cells treated for 24 hours. The MTT viability assay was employed. (Number of samples analyzed in triplicates, mean ± SD are shown)

The kinetics of release for Alendronate (ALD) from hollow Hydroxyapatite (HA) spheres were assessed in a Phosphate-buffered saline (PBS) solution adjusted to a pH of 7.4. Since the microspheres are designed for local delivery, they were placed in an environment resembling the extracellular space. As shown in **Figure 5**, ALD release was monitored over 5 days.

The results indicated linear release kinetics for the first few hours, followed by an initial burst release observed after 2 days across all three concentrations, with the highest burst release occurring at the 0.2 μM concentration, reaching 83.2%. This significant burst release may be due to the phenomenon of physical adsorption. Of

ALD onto the surface of the hollow HA microspheres (Mohanty *et al.*, 2012; Komatsu *et al.*, 2013), leading to a moderate and heterogeneous rate of drug loading.

In addition to that, the loading efficiency of ALD in the hollow HA microspheres at different strengths of 0.05 μM, 0.1 μM, and 0.2 μM was calculated and recorded between 44% and 48%. However, there was no substantial difference in the rate of ALD loaded among the hollow microspheres. To achieve better drug-loading efficiency, a more refined drug-loading process is necessary to ensure uniform drug distribution and controlled release kinetics.

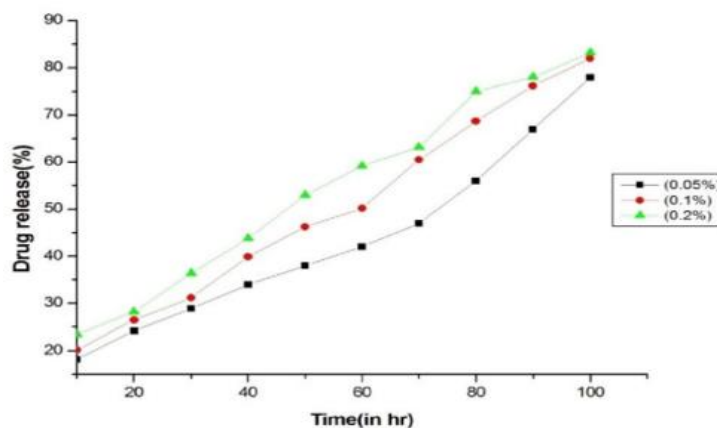


**Figure 5.** Controlled release of Alendronate (ALD) at various concentrations of 0.05, 0.1 and 0.2 μM from Hydroxyapatite (HA) Microspheres

**Conclusion**

In this study, we successfully developed Hydroxyapatite (HA) hollow microspheres for the localized delivery of Alendronate (ALD) using a simple template-directed method. This approach

features the physical adsorption of ALD onto the HA microspheres, enabling effective drug release. Characterization through FTIR and EDS confirmed the strong bonding between ALD anions and calcium cations in the calcium phosphate phase, enhancing the microspheres' suitability as drug carriers.

Cytotoxicity assessments showed that the tested concentrations of ALD (0.05  $\mu\text{M}$  to 0.2  $\mu\text{M}$ ) were non-cytotoxic to HT-1080 cells, indicating a favorable safety profile. Release kinetics revealed a linear profile with an initial burst phase, ensuring rapid availability of the drug for therapeutic action.

Overall, the ALD-HA hollow microspheres demonstrate potential as a local sustained delivery system, offering a promising alternative to existing oral formulations that experience low bioavailability. This innovative approach may improve treatment efficacy for conditions of bone health conditions, including osteoporosis and osteitis deformans (Paget's disease). Future research should focus on optimizing drug loading and validating in vivo applications to confirm clinical effectiveness.

**Acknowledgments:** The authors would like to thank the Management of Kampala International University, Uganda, and Malla Reddy University, Hyderabad for supporting this research work.

**Conflict of interest:** None

**Financial support:** None

**Ethics statement:** None

## References

- Agrawal, M., Gupta, S., Pich, A., Zafeiropoulos, N. E., & Stamm, M. (2009). A facile approach to fabrication of ZnO–TiO<sub>2</sub> hollow spheres. *Chemistry of Materials*, 21(21), 5343–5348.
- Agrawal, M., Pich, A., Zafeiropoulos, N. E., Gupta, S., Pionteck, J., Simon, F., & Stamm, M. (2007). Polystyrene–ZnO composite particles with controlled morphology. *Chemistry of Materials*, 19(7), 1845–1852.
- Boanini, E., Gazzano, M., Rubini, K., & Bigi, A. (2007). Composite nanocrystals provide new insight on alendronate interaction with hydroxyapatite structure. *Advanced Materials*, 19(18), 2499–2502.
- Boskey, A. L. (2013). Natural and synthetic hydroxyapatites. *Biomaterials Science an Introduction to Materials in Medicine, 3rd ed.; Ratner, BD, Hoffman, AS, Schoen, FJ, Lemons, JE, Eds*, 151–161.
- Bukke, S. P. N., Bharathi, A., Saraswathi, T. S., Nettikallu, Y., & Vippamakula, S. (2024). Formulation and evaluation of in-vitro anti-cancer activity of iron nanoparticles on MCF-7 & A-475 cells. *AUIQ Complementary Biological System*, 1(2), 21–30.
- Bukke, S. P. N., Himabindhu, P., Madhurameenakshi, C. H., Krishna, S. S., & Aishwarya, T. (2019). An overview on microspheres preparation and evaluation methods. *Indo American Journal of Pharmaceutical Research*, 9(11), 588–596. doi:10.5281/ZENODO.3559502
- Bukke, S. P. N., Venkatesh, C., Bandenahalli Rajanna, S., Saraswathi, T. S., Kusuma, P. K., Goruntla, N., Balasuramanyam, N., & Munishamireddy, S. (2024). Solid lipid nanocarriers for drug delivery: Design innovations and characterization strategies—A comprehensive review. *Discover Applied Sciences*, 6(6), 279.
- Cheng, T. L., Murphy, C. M., Cantrill, L. C., Mikulec, K., Carpenter, C., Schindeler, A., & Little, D. G. (2014). Local delivery of recombinant human bone morphogenetic proteins and bisphosphonate via sucrose acetate isobutyrate can prevent femoral head collapse in Legg-Calve-Perthes disease: A pilot study in pigs. *International Orthopaedics*, 38, 1527–1533.
- Chu, L. Y., Utada, A. S., Shah, R. K., Kim, J. W., & Weitz, D. A. (2007). Controllable monodisperse multiple emulsions. *Angewandte Chemie-International Edition in English*, 46(47), 8970.
- Crotts, G., & Park, T. G. (1995). Preparation of porous and nonporous biodegradable polymeric hollow microspheres. *Journal of Controlled Release*, 35(2-3), 91–105.
- Daryan, S. H., Khavandi, A., & Javadpour, J. (2020). Surface engineered hollow hydroxyapatite microspheres: Hydrothermal synthesis and growth mechanisms. *Solid State Sciences*, 106, 106301.
- Drake, M. T., Clarke, B. L., & Khosla, S. (2008). Bisphosphonates: Mechanism of action and role in clinical practice. In *Mayo clinic proceedings* (Vol. 83, No. 9, pp. 1032–1045). Elsevier.
- Glorieux, F. H. (2007). Experience with bisphosphonates in osteogenesis imperfecta. *Pediatrics*, 119(Supplement\_2), S163–S165.
- Goyal, M. R., & Kulkarni, S. (Eds.). (2024). *Advances in green and sustainable nanomaterials: Applications in energy, biomedicine, agriculture, and environmental science*, 1 ed. Palm Bay, FL: Apple Academic Press.
- Im, G. I., Qureshi, S. A., Kenney, J., Rubash, H. E., & Shanbhag, A. S. (2004). Osteoblast proliferation and maturation by bisphosphonates. *Biomaterials*, 25(18), 4105–4115.
- Jagyanseni, S., Mishra, S., & Sahoo, S. N. (2023). A study on genotoxic potential of acephate in *Clarias batrachus*. *Journal for Research in Applied Sciences and Biotechnology*, 2(1), 22–25.
- Josse, S., Fauchoux, C., Soueidan, A., Grimandi, G., Massiot, D., Alonso, B., Janvier, P., Laïb, S., Pilet, P., Gauthier, O., et al. (2005). Novel biomaterials for bisphosphonate delivery. *Biomaterials*, 26(14), 2073–2080.
- Komatsu, K., Shimada, A., Shibata, T., Wada, S., Ideno, H., Nakashima, K., Amizuka, N., Noda, M., & Nifuji, A. (2013). Alendronate promotes bone formation by inhibiting protein prenylation in osteoblasts in rat tooth replantation model. *The Journal of Endocrinology*, 219(2), 145–158.
- Kuboki, Y., Takita, H., Kobayashi, D., Tsuruga, E., Inoue, M., Murata, M., Nagai, N., Dohi, Y., & Ohgushi, H. (1998). BMP-induced osteogenesis on the surface of hydroxyapatite with geometrically feasible and nonfeasible structures: Topology of osteogenesis. *Journal of Biomedical Materials Research: An Official Journal of the Society for Biomaterials, The Japanese Society for Biomaterials, and the Australian Society for Biomaterials*, 39(2), 190–199.
- Kumar, A., Nune, K. C., & Misra, R. D. K. (2016). Biological functionality of extracellular matrix-ornamented three-dimensional printed hydroxyapatite scaffolds. *Journal of Biomedical Materials Research Part A*, 104(6), 1343–1351.
- Lou, X. W., Yuan, C., & Archer, L. A. (2007). Shell-by-shell synthesis of tin oxide hollow colloids with

- nanoarchitected walls: Cavity size tuning and functionalization. *Small*, 3(2), 261-265.
- Meldrum, F. C., & Cölfen, H. (2008). Controlling mineral morphologies and structures in biological and synthetic systems. *Chemical Reviews*, 108(11), 4332-4432.
- Mohanty, S., Mishra, S., Jena, P., Jacob, B., Sarkar, B., & Sonawane, A. (2012). An investigation on the antibacterial, cytotoxic, and antibiofilm efficacy of starch-stabilized silver nanoparticles. *Nanomedicine: Nanotechnology, Biology and Medicine*, 8(6), 916-924.
- Orcel, P., & Beaudreuil, J. (2002). Bisphosphonates in bone diseases other than osteoporosis. *Joint Bone Spine*, 69(1), 19-27.
- Sarma, K. N., Thalluri, C., & Mandhadi, J. R. (2024). Nanofibers in drug delivery systems: A comprehensive scientific review of recent approaches. *International Journal of Pharmaceutical Investigation*, 14(3), 633-646.
- Slowing, I. I., Trewyn, B. G., Giri, S., & Lin, V. Y. (2007). Mesoporous silica nanoparticles for drug delivery and biosensing applications. *Advanced Functional Materials*, 17(8), 1225-1236.
- Sparidans, R. W., Twiss, I. M., & Talbot, S. (1998). Bisphosphonates in bone diseases. *Pharmacy World and Science*, 20, 206-213.
- Srujan, B., Chandrashekar, T., Swathi, A., & Sunil, R. (2018). Design and in-vitro evaluation of controlled release tablets of tramadol hydrochloride. *American Journal of PharmTech Research*, 8, 115-124.
- Tamber, H., Johansen, P., Merkle, H. P., & Gander, B. (2005). Formulation aspects of biodegradable polymeric microspheres for antigen delivery. *Advanced Drug Delivery Reviews*, 57(3), 357-376.
- Thalluri, C. (2024). Exploring adsorption phenomena in pharmaceutical formulation design: A systematic quality-by-design approach for agomelatine-loaded liquid compact tablets. *Asian Journal of Pharmaceutics (AJP)*, 18(01).
- Thalluri, C. S., Bontha, V. K., & Devanna, N. (2013). Enhancement of Entacapone bioavailability by polymorphism. *International Journal of Pharmacy and Technology*, 5, 5753-5760.
- Thalluri, C., Bontha V., & Devanna, N. (2014). Polymorphism of Lomefloxacin: Preparation, characterisation and evaluation of its anti-microbial activity. *International Journal of Pharmacy and Biological Science*, 4(3), 126-132.
- Thalluri, C., Swain, K., & Pattnaik, S. (2023). Rise of gold nanoparticles as carriers of therapeutic agents. *Acta Chimica Slovenica*, 70(4), 467-478.
- Umegaki, T., Watanabe, K., Ogawa, H., & Kojima, Y. (2020). Influence of swelling agents on pore size distributions of porous silica-alumina hollow sphere particles in acid-promoted hydrolytic generation of hydrogen from ammonia borane. *International Journal of Hydrogen Energy*, 45(38), 19531-19538.
- Vasam, M., Maddiboyina, B., Talluri, C., Alagarsamy, S., Gugulothu, B., & Roy, H. (2023). Formulation, characterization, and Taguchi design study of eplerenone lipid-based solid dispersions integrated with gelucire. *BioNanoScience*, 13(2), 576-587.
- Wu, S., Liu, X., Hu, T., Chu, P. K., Ho, J. P. Y., Chan, Y. L., Yeung, K. W. K., Chu, C. L., Hung, T. F., Huo, K. F., et al. (2008). A biomimetic hierarchical scaffold: Natural growth of nanotitanates on three-dimensional microporous Ti-based metals. *Nano Letters*, 8(11), 3803-3808.
- Xiong, Y., Yang, H. J., Feng, J., Shi, Z. L., & Wu, L. D. (2009). Effects of alendronate on the proliferation and osteogenic differentiation of MG-63 cells. *Journal of International Medical Research*, 37(2), 407-416.
- Yang, L. J., Shen, F. X., Zheng, J. C., & Zhang, H. L. (2012). Clinical application of alendronate for osteoporosis/osteopenia secondary to hyperthyroidism. *Zhongguo gu Shang= China Journal of Orthopaedics and Traumatology*, 25(2), 133-137.
- Yi, L., Feng, J., Qin, Y. H., & Li, W. Y. (2017). Prediction of elemental composition of coal using proximate analysis. *Fuel*, 193, 315-321.
- Zhang, Z., Shao, X., Yu, H., Wang, Y., & Han, M. (2005). Morphosynthesis and ornamentation of 3D dendritic nanoarchitectures. *Chemistry of Materials*, 17(2), 332-336.
- Zhong, L. S., Hu, J. S., Cao, A. M., Liu, Q., Song, W. G., & Wan, L. J. (2007). 3D flowerlike ceria micro/nanocomposite structure and its application for water treatment and CO removal. *Chemistry of Materials*, 19(7), 1648-1655.
- Zhou, L., Hu, Z., Li, H. Y., Liu, J., Zeng, Y., Wang, J., Huang, Y., Miao, L., Zhang, G., Huang, Y., et al. (2021). Template-free construction of tin oxide porous hollow microspheres for room-temperature gas sensors. *ACS Applied Materials & Interfaces*, 13(21), 25111-25120.